

# Active Targeting of Tumors through Conformational Epitope Imprinting\*\*

Yan Zhang, Chunyue Deng, Sha Liu, Jin Wu, Zhangbao Chen, Chong Li,\* and Weiyue Lu

**Abstract:** Inspired by the knowledge that most antibodies recognize a conformational epitope because of the epitope's specific three-dimensional shape rather than its linear structure, we combined scaffold-based peptide design and surface molecular imprinting to fabricate a novel nanocarrier harboring stable binding sites that captures a membrane protein. In this study, a disulfide-linked  $\alpha$ -helix-containing peptide, apamin, was used to mimic the extracellular, structured N-terminal part of the protein p32 and then serve as an imprinting template for generating a sub-40 nm-sized polymeric nanoparticle that potently binds to the target protein, recognizes p32-positive tumor cells, and successfully mediates targeted photodynamic therapy in vivo. This could provide a promising alternative for currently used peptide-modified nanocarriers and may have a broad impact on the development of polymeric nanoparticle-based therapies for a wide range of human diseases.

**A**ctive tumor/cancer-targeting drug delivery is a tumor-treatment strategy that improves tumor-cell-specific uptake of drug molecules with enhanced therapeutic efficacy. This strategy entails specific recognition of the surface marker of a tumor cell by a ligand either directly conjugated to the drug molecule or fabricated on a vehicle containing it.<sup>[1]</sup> The targeting ligands can be small molecules as well as macromolecules such as peptides and proteins.<sup>[2]</sup> Unlike a small-molecule ligand, a peptide or protein ligand enjoys superior specificity and high affinity for tumor markers; however, it

often suffers poor in vivo stability, immunogenicity, and high costs of production.<sup>[3]</sup> Novel chemistries are needed to design therapeutically viable ligands for anticancer drug delivery that share the best features of both small molecules and macromolecules.

Molecular imprinting refers to a technology that embeds a template molecule in polymer matrices, thereby creating cavities. After template dissociation, the shape of the template is not only retained, but the polymer also specifically recognizes it. This technology has been successfully used for constructing various polymer materials that bind specifically to peptide and protein templates, providing a promising tool for molecular design, drug discovery, and drug delivery.<sup>[4,5]</sup> The early practitioners of molecular imprinting techniques focus primarily on the use of short linear peptides as template molecules, limiting their applications to the few biological systems in which the recognition of linear epitopes prevails. It has been challenging to develop imprinted polymer materials that recognize the conformational epitope of a protein—the mode of recognition that predominates in biology. Here, we report the design of a novel magic bullet that specifically recognizes the tumor cell membrane protein targets as a result of the combination of surface molecular imprinting and scaffold-based peptide design (Scheme 1).

The membrane protein p32, which is also named gC1qR or HABP1, was recently shown to be overexpressed on the surface of a variety of tumor cells and, therefore, to be capable of mediating targeted drug delivery to tumor sites.<sup>[6]</sup> The extracellular domain of mature p32, which harbors an N-terminal  $\alpha$ -helix, served as the binding site for a specific ligand that recognized p32 and even entire tumor cells expressing p32.<sup>[7]</sup> Previously, we and others successfully used an  $\alpha$ -helix-containing disulfide-bridged peptide derived from bee venom, apamin, as a scaffold for designing novel peptides that mimic other functional protein domains featuring similar structures.<sup>[8]</sup> In this study, the dispersed residues located in the N-terminal  $\alpha$ -helix of p32 (including <sup>79</sup>D, <sup>81</sup>A, <sup>82</sup>F, <sup>83</sup>V, <sup>85</sup>F, <sup>86</sup>L, and <sup>87</sup>S) were grafted into the corresponding site of apamin (including <sup>10</sup>L, <sup>12</sup>A, <sup>13</sup>R, <sup>14</sup>R, <sup>16</sup>Q, <sup>17</sup>Q, and <sup>18</sup>H); the original apamin residues were replaced with topologically equivalent residues from p32, but the ninth alanine that exhibits the highest  $\alpha$ -helix propensity and two cysteines were retained. The produced peptide, HAPPE (hybrid apamin-p32 polypeptide), possessed the novel integrated sequence CNCKAPET-ADCAFCVCLF, with seven residues being identical to the corresponding residues of p32, which meets the requirement for epitope imprinting,<sup>[9]</sup> and the peptide almost maintained the exact featured structure stabilized by two disulfide bonds (see the Supporting Information, Figure S1). A palmitic acid was conjugated to the free amino group of the fourth lysine in

[\*] Y. Zhang,<sup>[a]</sup> C. Deng,<sup>[a]</sup> S. Liu, J. Wu, Prof. Dr. Z. Chen, Prof. Dr. C. Li  
Key Laboratory of Luminescence and Real-time Analytical Chemistry  
(Ministry of Education)

College of Pharmaceutical Sciences, Southwest University  
No. 2 Tiansheng Road, Beibei, Chongqing 400715 (China)  
E-mail: chongli2009@gmail.com

Prof. Dr. Z. Chen, Prof. Dr. C. Li  
Chongqing Engineering Research Center for Pharmaceutical Pro-  
cess and Quality Control (China)

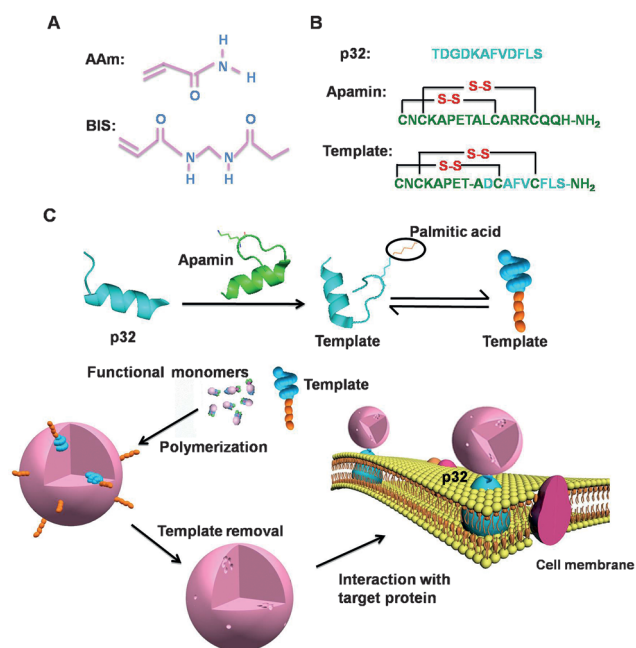
Prof. W. Lu  
Key Laboratory of Smart Drug Delivery (Ministry of Education)  
School of Pharmacy, Fudan University  
Shanghai 201203 (China)

[†] These authors contributed equally to this work.

[\*\*] This work was supported by the National Basic Research Program of China (973 Program) 2013CB932500, National Natural Science Foundation of China (numbers 81102404 and 21272187), the Fundamental Research Funds for the Central Universities (XDJK2013A010, XDJK2013A015), and the Program for Innovative Research Team in University of Chongqing (2013).



Supporting information for this article is available on the WWW under <http://dx.doi.org/10.1002/anie.201412114>.



**Scheme 1.** Molecularly imprinted polymeric nanoparticles designed for specifically recognizing a membrane protein.

case the imprinted  $\alpha$ -helix domain localized at the developing water-polymer interface during polymerization.<sup>[10]</sup> Acrylamide (AAm) and *N,N'*-methylenebisacrylamide (BIS) were used as functional monomers and the molecularly imprinted polymeric nanoparticles (MIPNPs) were synthesized using inverse microemulsion polymerization as described.<sup>[10]</sup> The obtained nanoparticles exhibited a uniform particle size of approximately 37 nm and a narrow size distribution (Figure S2).

We used the fluorescence polarization (FP) technique to quantify the interaction of MIPNPs with recombinant p32.<sup>[11,12]</sup> Both direct titration and competitive binding assays have demonstrated that MIPNPs bind strongly to p32 protein (Figures 1 A,B and S3A). The results of other experiments showed that as compared with NIPNPs, MIPNPs exhibited no specific binding to phospholipase A2, which possesses an N-terminal  $\alpha$ -helix, or to other proteins such as mouse nerve growth factor (NGF; Figure S3B).<sup>[13]</sup> In a further

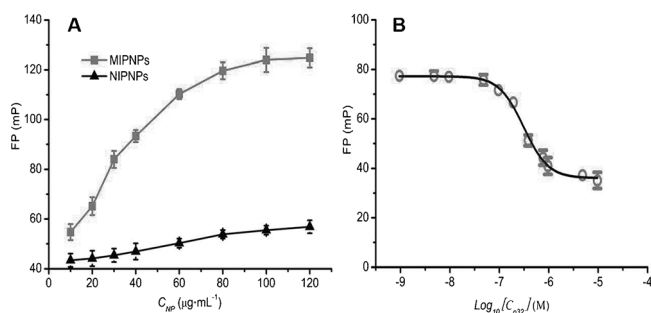


**Figure 1.** A) Fluorescence polarization experiment used for examining direct binding between MIPNPs and p32.  $\blacktriangle$  MIPNPs; and  $\blacksquare$  NIPNPs (non-imprinted nanoparticles). B) Competitive binding assays. The  $IC_{50}$  of free p32 was calculated to be 340 nM.

step, we incubated MIPNPs encapsulating 6-aminofluorescein (FAM, a fluorescence probe) with two p32-positive cancer cells, 4T1 murine breast cancer cells and BxPC-3 human pancreatic cancer cells, and maintained the cells at 37°C for a predetermined time.<sup>[14]</sup> The results of flow cytometry assays showed that both types of cancer cells exhibited substantially higher uptake of MIPNPs than of NIPNPs (Figure 2 A,B).

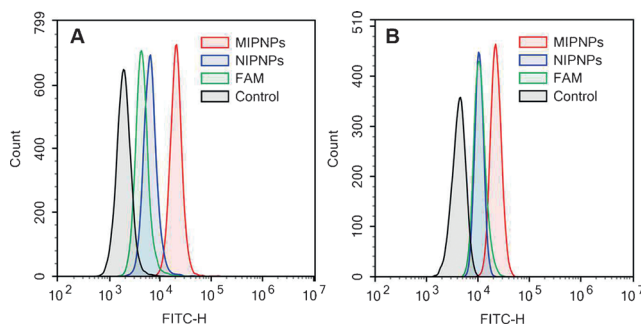


**Figure 2.** Flow cytometric measurement of the cellular uptake of FAM-loaded NPs by target cells. A) 4T1 cells; B) BxPC-3 cells. Green curves: free FAM; black curves: the cells alone.

After incubation for 2 h, the fluorescence intensity of MIPNP-treated 4T1 cancer cells was nearly three times higher than that of NIPNP-treated cells. Moreover, no clear decrease in cellular uptake of MIPNPs was detected when the nanoparticles were preincubated with serum for 1 h and then incubated with target cells (Figure S4), which suggests a stable, cancer-specific targeting of the nanoparticles in a complex environment.

Furthermore, we established a xenograft mouse model of cancer to evaluate the targeting capability of MIPNPs *in vivo*. Our results showed that intravenous administration of nanoparticles encapsulating a near-infrared fluorophore (IR-783 dye) led to considerably higher accumulation in tumors of MIPNPs than of NIPNPs in the mouse xenograft 4T1 tumor model (Figure 3 A–C). More importantly, the distribution in tumor sites of MIPNPs was greatly diminished following a 30 min pre-injection in the peritumor region of Lyp-1, a peptide ligand that by phage-display screening was shown to bind to the N-terminal domain of p32; this result indicates that specific interactions between MIPNPs and p32 were mainly responsible for the active tumor targeting of the nanoparticles (Figure 3A). A similar positive trend was observed in the case of the poorly permeable BxPC-3 pancreatic xenograft model (Figure S5).<sup>[15]</sup> Lastly, an even more promising finding was that in brain tissues infiltrated by intracranially implanted p32-positive breast cancer cells, MIPNPs accumulated more effectively than did the non-imprinted nanoparticles (Figure S6). These *in vivo* imaging studies strongly suggested that this sub-40 nm-sized, surface molecularly imprinted nanoparticle could serve as an efficient magic bullet for tracking p32-positive tumors *in vivo* and for efficiently penetrating physiological barriers.

In recent years, polyacrylamide nanoparticles (PAA-NPs) have been reported to function as effective carriers of

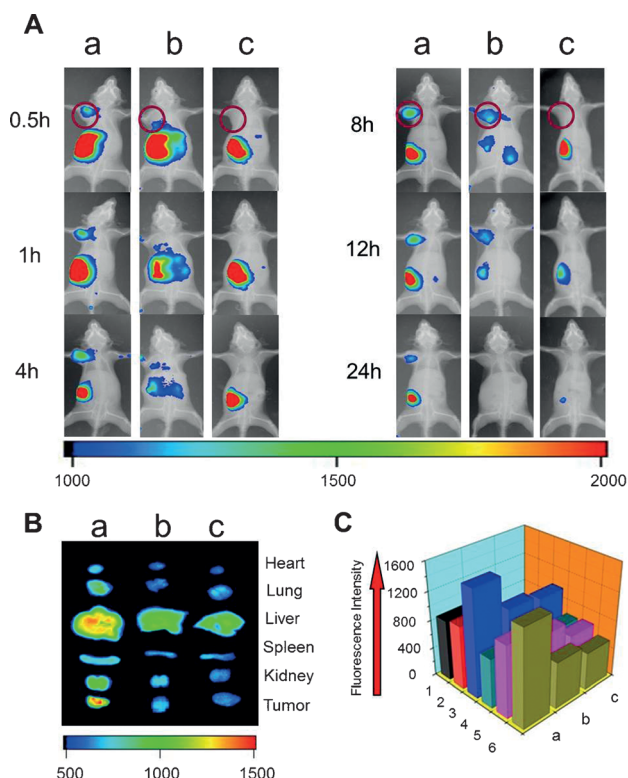


**Figure 3.** In vivo distribution of nanoparticles in 4T1-tumor-bearing mice. A) The 4T1-tumor-bearing KM mice were intravenously injected with various nanoparticles. B) The organs and tumors were examined at 24 h. C) Semiquantitative results obtained using fluorescence imaging for ex vivo hearts (1), lungs (2), livers (3), spleens (4), kidneys (5), and tumors (6); nanoparticles: a) MIPNPs, b) Lyp-1 + MIPNPs, c) NIPNPs.

photosensitive agents and thus serve as useful drug-delivery vehicles in photodynamic therapy.<sup>[16]</sup> Notably, hydrophilic photosensitive agents can be loaded into PAA-NPs through inverse microemulsion polymerization, a step similar to the step used for generating imprinted PAA-NPs. Thus, we tested whether the surface-molecular-imprinting and drug-loading steps could be combined and used concurrently, and our results demonstrated that this was possible. We prepared MIPNPs ( $1 \text{ mg mL}^{-1}$ ) loaded with the photosensitizer methylene blue (MB,  $3 \mu\text{M}$ ) in a manner identical to blank nanoparticles except that we added MB into the water phase before polymerization.<sup>[17]</sup> As per our expectation, photodynamic treatment (PDT) performed subsequently showed that MB-encapsulating MIPNPs more potently inhibited cancer in the 4T1 subcutaneous xenografts than did the nonimprinted nanoparticles. These results agreed well with the results of cellular ROS (reactive oxygen species) production assays (Figures 4 and S7B). Furthermore, the results of both cell toxicity assays and pathological analysis of tissue sections demonstrated high biocompatibility of the prepared PAA-NPs (Figures S7A and S8).

Recently, we developed apamin-modified nanomicelles for active targeted therapy of spinal cord injury by using its unique avidity toward the central neural system, especially the spinal cord.<sup>[18]</sup> Before designing HAPPE, we explored

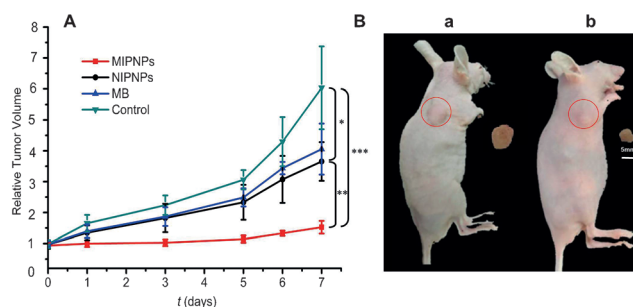


**Figure 4.** A) In vivo antitumor effect of PDT performed using distinct nanoparticle formulations. All injections were performed once at  $t=0$ . Tumor volumes were measured every other day for one week;  $*P < 0.05$ ,  $**P < 0.01$ ,  $***P < 0.005$ . B) Images of mice treated with NIPNPs (a) and MIPNPs (b). Scale bar = 5 mm.

whether apamin itself could be used as the imprinting template. The synthesized polymeric nanoparticles strongly bound to apamin (Figure S9), and the specificity of this recognition of apamin by the nanoparticles in vivo was demonstrated by the neutralization of apamin by the nanoparticles. In spinal cord tissues, we observed a markedly reduced distribution of FITC-labeled apamin following either intravenous administration of a preincubated mixture of the nanoparticles and apamin or sequential injection of nanoparticles and apamin (Figure S10). Moreover, the imprinted nanoparticles functioned as a “defense system” and neutralized the “launched” apamin-modified micelles in vivo, regardless of whether the micelles were administered before or after the nanoparticles (Figures S11 and S12). Notably, synthetic polymeric nanoparticles that were prepared using a linear analogue of apamin (in which four cysteines were changed to alanines) as the imprinting template exhibited an extremely low response to apamin as compared with the nanoparticles prepared using apamin as the template. Similarly, synthetic polymeric nanoparticles generated using a linear analogue of HAPPE (four cysteines replaced with alanines) as the imprinting template were poorly taken up by p32-positive cancer cells. They were accumulated at low levels in subcutaneously implanted tumors and were only slightly different from the nonimprinted controls (Figure S13). These results indicated that consistency in the secondary structure between the imprinted template and the target peptide is more critical than consistency in the primary sequence for achieving potent binding between a molecularly imprinted polymer and its corresponding target.

Biomedical application has served for decades as one of the major research areas in which molecular imprinting technology has been used.<sup>[19]</sup> With regard to drug delivery in particular, early efforts using the drug itself as an imprinting template led to the successful design of novel controlled-release delivery systems.<sup>[20]</sup> The next step was to construct specified delivery systems to achieve selective drug targeting through molecular imprinting. Not unexpectedly, membrane proteins were considered as the main targets because they represent a major class of disease biomarkers that are located on the surface of target cells. The epitope-imprinting strategy has provided a highly favorable starting point to achieve the



capture of partially exposed transmembrane proteins. The next key point in fabricating antibody-like nanoparticles directed against membrane proteins is the selection of suitable “epitopes”, because most antibodies recognize and potentially bind to conformational epitopes as a result of the specific three-dimensional shape of the epitopes rather than their linear structure.

In this study, we developed a novel strategy named conformational epitope imprinting, in which the central focus is on the selection of specific structured regions of target proteins combined with the mimicking of structures by using peptide scaffolds. This conformational epitope imprinting method could have great potential for further use in the recognition of other proteins, especially proteins that possess conformational epitopes composed of noncontiguous sequences. Moreover, the ability to functionalize imprinted nanoparticles<sup>[21]</sup> will likely lead to the creation of additional “smart” nanocarriers for biomedical applications in which conformational epitope imprinting is coupled with the use of synthetic polymeric nanoparticles. Other new ideas that could be investigated in future studies involve the design of “polymeric drugs” or drug-free polymeric therapeutics in which the nanoparticles themselves antagonize specific ligand–receptor interactions.

In conclusion, we have presented a conformational epitope imprinting strategy to construct a novel tumor-targeted drug-delivery system; in this strategy, the functional peptide has mediated tumor targeting in a totally different way than the currently used peptide-modified nanocarriers. This work may have a broad impact on the development of polymeric nanoparticle-based targeted diagnoses and therapies used for a great variety of human diseases.

**Keywords:** conformational epitopes · drug delivery · imprinting · photodynamic therapy · tumor targeting

**How to cite:** *Angew. Chem. Int. Ed.* **2015**, *54*, 5157–5160  
*Angew. Chem.* **2015**, *127*, 5246–5249

- [1] a) Y. H. Bae, K. Park, *J. Controlled Release* **2011**, *153*, 198–205; b) T. Lammers, F. Kiessling, W. E. Hennink, G. Storm, *J. Controlled Release* **2012**, *161*, 175–187.
- [2] a) Z. Yu, R. M. Schmaltz, T. C. Bozeman, R. Paul, M. J. Rishel, K. S. Tsosie, S. M. Hecht, *J. Am. Chem. Soc.* **2013**, *135*, 2883–2886; b) Y. Zhong, F. Meng, C. Deng, Z. Zhong, *Biomacromolecules* **2014**, *15*, 1955–1969.
- [3] C. Li, Y. Wang, X. Zhang, L. Deng, Y. Zhang, Z. Chen, *Int. J. Nanomed.* **2013**, *8*, 1051–1062.
- [4] a) M. J. Whitcombe, I. Chianella, L. Larcombe, S. A. Piletsky, J. Noble, R. Porter, A. Horgan, *Chem. Soc. Rev.* **2011**, *40*, 1547–1571; b) S. Shinde, A. Bunschoten, J. A. Kruijtzter, R. M. Liskamp, B. Selligren, *Angew. Chem. Int. Ed.* **2012**, *51*, 8326–8329; *Angew. Chem.* **2012**, *124*, 8451–8454; c) G. Vlatakis, L. I. Andersson, R. Müller, K. Mosbach, *Nature* **1993**, *361*, 645–647; d) J. Svenson, N. Zheng, I. A. Nicholls, *J. Am. Chem. Soc.* **2004**, *126*, 8554–8560.
- [5] a) T. Akiyama, T. Hishiya, H. Asanuma, M. Komiyama, *J. Inclusion Phenom. Macrocyclic Chem.* **2001**, *41*, 149–153; b) P. Çakir, A. Cutivet, M. Resmini, B. T. Bui, K. Haupt, *Adv. Mater.* **2013**, *25*, 1048–1051; c) X. Shen, J. Svensson Bonde, T. Kamra, L. Bülow, J. C. Leo, D. Linke, L. Ye, *Angew. Chem. Int. Ed.* **2014**, *53*, 10687–10689; *Angew. Chem.* **2014**, *126*, 10863–10866.
- [6] V. Fogal, L. Zhang, S. Krajewski, E. Ruoslahti, *Cancer Res.* **2008**, *68*, 7210–7218.
- [7] a) J. Jiang, Y. Zhang, A. R. Krainer, R. M. Xu, *Proc. Natl. Acad. Sci. USA* **1999**, *96*, 3572–3577; b) P. Laakkonen, M. E. Åkerman, H. Biliran, M. Yang, F. Ferrer, T. Karpanen, R. M. Ferrer, E. Ruoslahti, *Proc. Natl. Acad. Sci. USA* **2004**, *101*, 9381–9386; c) Z. Yan, F. Wang, Z. Wen, C. Zhan, L. Feng, Y. Liu, X. Wei, C. Xie, W. Lu, *J. Controlled Release* **2012**, *157*, 118–125.
- [8] a) J. H. Pease, R. W. Storrs, D. E. Wemmer, *Proc. Natl. Acad. Sci. USA* **1990**, *87*, 5643–5647; b) A. J. Nicoll, D. J. Miller, K. Fütterer, R. Ravelli, R. K. Allemann, *J. Am. Chem. Soc.* **2006**, *128*, 9187–9193; c) C. Li, M. Pazgier, M. Liu, W. Y. Lu, W. Lu, *Angew. Chem. Int. Ed.* **2009**, *48*, 8712–8715; *Angew. Chem.* **2009**, *121*, 8868–8871.
- [9] a) A. Rachkov, N. Minoura, *J. Chromatogr. A* **2000**, *889*, 111–118; b) H. Nishino, C. S. Huang, K. J. Shea, *Angew. Chem. Int. Ed.* **2006**, *45*, 2392–2396; *Angew. Chem.* **2006**, *118*, 2452–2456.
- [10] Z. Zeng, Y. Hoshino, A. Rodriguez, H. Yoo, K. J. Shea, *ACS Nano* **2010**, *4*, 199–204.
- [11] a) S. Dédier, S. Reinelt, S. Rion, G. Folkers, D. Rognan, *J. Immunol. Methods* **2001**, *255*, 57–66; b) S. Kota, C. Coito, G. Mousseau, J. P. Lavergne, A. D. Strosberg, *J. Gen. Virol.* **2009**, *90*, 1319–1328; c) C. Li, C. Zhan, L. Zhao, X. Chen, W. Y. Lu, W. Lu, *Bioorg. Med. Chem.* **2013**, *21*, 4045–4050.
- [12] Y. Hoshino, T. Kodama, Y. Okahata, K. J. Shea, *J. Am. Chem. Soc.* **2008**, *130*, 15242–15243.
- [13] K. Sekar, *Curr. Top. Med. Chem.* **2007**, *7*, 779–785.
- [14] a) L. Roth, L. Agemy, V. R. Kotamraju, G. Braun, T. Teesalu, K. N. Sugahara, J. Hamzah, E. Ruoslahti, *Oncogene* **2012**, *31*, 3754–3763; b) G. Luo, X. Yu, C. Jin, F. Yang, D. Fu, J. Long, J. Xu, C. Zhan, W. Lu, *Int. J. Pharm.* **2010**, *385*, 150–156.
- [15] H. Cabral, Y. Matsumoto, K. Mizuno, Q. Chen, M. Murakami, M. Kimura, Y. Terada, M. R. Kano, K. Miyazono, M. Uesaka, N. Nishiyama, K. Kataoka, *Nat. Nanotechnol.* **2011**, *6*, 815–823.
- [16] M. Qin, H. J. Hah, G. Kim, G. Nie, Y. E. Lee, R. Kopelman, *Photochem. Photobiol. Sci.* **2011**, *10*, 832–841.
- [17] a) W. Tang, H. Xu, E. J. Park, M. A. Philbert, R. Kopelman, *Biochem. Biophys. Res. Commun.* **2008**, *369*, 579–583; b) M. Kurupparachchi, H. Savoie, A. Lowry, C. Alonso, R. W. Boyle, *Mol. Pharm.* **2011**, *8*, 920–931.
- [18] a) F. J. van der Staay, R. J. Fanelli, A. Blokland, B. H. Schmidt, *Neurosci. Biobehav. Rev.* **1999**, *23*, 1087–1110; b) J. Wu, H. Jiang, Q. Bi, Q. Luo, J. Li, Y. Zhang, Z. Chen, C. Li, *Mol. Pharm.* **2014**, *11*, 3210–3222.
- [19] a) G. Wulff, *Angew. Chem. Int. Ed. Engl.* **1995**, *34*, 1812–1832; *Angew. Chem.* **1995**, *107*, 1958–1979; b) A. L. Hillberg, K. R. Brain, C. J. Allender, *Adv. Drug Delivery Rev.* **2005**, *57*, 1875–1889; c) T. Takeuchi, T. Mori, A. Kuwahara, T. Ohta, A. Oshita, H. Sunayama, Y. Kitayama, T. Ooya, *Angew. Chem. Int. Ed.* **2014**, *53*, 12765–12770; *Angew. Chem.* **2014**, *126*, 12979–12984; d) W. Bai, D. A. Spivak, *Angew. Chem. Int. Ed.* **2014**, *53*, 2095–2098; *Angew. Chem.* **2014**, *126*, 2127–2130.
- [20] J. Z. Hilt, M. E. Byrne, *Adv. Drug Delivery Rev.* **2004**, *56*, 1599–1620.
- [21] a) N. Pérez-Moral, A. G. Mayes, *Macromol. Rapid Commun.* **2007**, *28*, 2170–2175; b) P. K. Ivanova-Mitseva, A. Guerreiro, E. V. Piletska, M. J. Whitcombe, Z. Zhou, P. A. Mitsev, F. Davis, S. A. Piletsky, *Angew. Chem. Int. Ed.* **2012**, *51*, 5196–5199; *Angew. Chem.* **2012**, *124*, 5286–5289.

Received: December 18, 2014

Published online: February 26, 2015